JVST A
Journal of Vacuum Science & Technology A

In situ ellipsometry aided rapid ALD process development and parameter space visualization of cerium oxide nanofilms

Cite as: J. Vac. Sci. Technol. A **39**, 060405 (2021); https://doi.org/10.1116/6.0001329
Submitted: 02 August 2021 • Accepted: 29 September 2021 • Published Online: 02 November 2021

Udit Kumar, Corbin Feit, S. Novia Berriel, et al.

JVST A
Journal of Vacuum Science & Technology A

LETTER

avs.scitation.org/journal/jva

In situ ellipsometry aided rapid ALD process development and parameter space visualization of cerium oxide nanofilms

Cite as: J. Vac. Sci. Technol. A **39**, 060405 (2021); doi: 10.1116/6.0001329
Submitted: 2 August 2021 · Accepted: 29 September 2021 ·
Published Online: 2 November 2021

Udit Kumar,[1,2,b)] Corbin Feit,[2,b)] S. Novia Berriel,[2] Ayush Arunachalam,[4] Tamil Selvan Sakthivel,[1,2] Kanad Basu,[4] Parag Banerjee,[2,3,5,6,a)] and Sudipta Seal[1,2,3,7,a)]

AFFILIATIONS

[1]Advanced Materials Processing and Analysis Center, University of Central Florida, Orlando, Florida 32816
[2]Department of Materials Science and Engineering, University of Central Florida, Orlando, Florida 32816
[3]Nanoscience Technology Center, University of Central Florida, Orlando, Florida 32816
[4]Department of Electrical and Computer Engineering, The University of Texas at Dallas, Richardson, Texas 75080
[5]Renewable Energy and Chemical Transformation (REACT) Faculty Cluster, University of Central Florida, Orlando, Florida 32816
[6]Florida Solar Energy Center (FSEC), University of Central Florida, Orlando, Florida 32922
[7]College of Medicine, University of Central Florida, Orlando, Florida 32827

[a)]**Authors to whom correspondence should be addressed:** sudipta.seal@ucf.edu and parag.banerjee@ucf.edu
[b)]Equal contribution

ABSTRACT

Process development in atomic layer deposition (ALD) is often time-consuming, requiring optimization of saturation curves and temperature windows for controlled deposition rates. Any ALD process should be self-limiting in nature, exhibiting a temperature window of nominal deposition and a linear deposition rate. Meeting these criteria usually requires several ALD experiments, followed by film characterization, which are generally time, cost, and labor-intensive. Against this backdrop, we report a methodology using *in situ* ellipsometry to rapidly develop the ALD process for cerium oxide using $Ce(iPrCp)_2(N\text{-}iPr\text{-}amd)$ and water. The entire optimized process was realized in ten experiments of sequential pulsing as a function of temperature, requiring less than a day. In the traditional approach, tens of experiments and *ex situ* characterization may be required. The approach reported here generated a contour visualization of the time-temperature-thickness parameter space delineating the optimal deposition conditions. The cerium oxide deposition rate deposited in the ALD temperature window was ~0.15 nm/cycle; the deposited film was further characterized using x-ray photoelectron spectroscopy, x-ray diffraction, and atomic force microscopy to probe the film composition and quality further.

I. INTRODUCTION

The expanding portfolio of material chemistries (metals, oxides, and composites) and the vast applicability of ultrathin films have denoted atomic layer deposition (ALD) as a preferred deposition method among several industries.[1–6] It is estimated that ALD will reach a market value of $3.01 billion by 2025 (grandviewresearch.com, Report ID: GVR-2-68038-215-0). ALD consists of alternating pulses of gaseous precursors via a self-limiting chemisorption mechanism on the surface of a substrate to form sequential monolayers of a film. The self-limiting nature of ALD enables the deposition of thin films with precise thickness and compositional control.[7] Furthermore, ALD is particularly effective on high aspect ratio surfaces compared to traditional vapor deposition techniques [e.g., chemical vapor deposition (CVD)].[7]

With the growing demand for new ALD processes comes the need for rapid process development and diagnostics to aid integration into industrial manufacturing. An ALD process must satisfy three defining characteristics of the deposition rate. First, a self-limiting nature of deposition that is independent of the pulse time of the precursor (saturation curve). Second, a temperature window that exhibits the stable deposition rate (temperature window). Third, a linear deposition rate. The development of ALD processes

requires independently defining process parameters such as pressure, the temperature of the delivery lines and reactor, flow rates of various gases/precursors, and pulse and purge times. These parameters determine the deposition rate (thickness/cycle), crystallinity, chemical composition (oxidation/vacancies), phase, dielectric constant (insulators), conductivity (metals), optical properties, etc. Saturation curves, deposition rate, and temperature window are typically defined by a series of experiments that assess each parameter independently. *Ex situ* methodologies are time-consuming and lack transparency on how secondary independent parameters affect the deposition process.

On the other hand, *in situ* characterization techniques have been employed to extract real-time information about the ALD process through quartz crystal microbalance (QCM),[8–12] quadrupole mass spectrometry,[8,9,12,13] Fourier transform infrared spectroscopy,[11,14] x-ray photoemission spectroscopy (XPS),[15] optical emission spectroscopy,[12,14,16] and spectroscopic ellipsometry (SE).[16–19] While the mentioned *in situ* techniques provide essential information about the surface chemistry reactions and film properties, *in situ* SE provides critical information such as the deposition rate and saturation submonolayers; nucleation behavior; and optical, phase, composition, and electrical properties.[17] The methodology of SE has been used to develop complicated ALD chemistries. This technique measures the change in the polarization of a light beam (~180–1690 nm) reflected from a surface given by the amplitude ratio Y and phase angle D. The data are fit using known or derived optical constants to extract the physical information (i.e., thickness) of the thin film. Langereis *et al.* provided a comprehensive review on *in situ* SE with ALD,[17,19] and others have reported on the *in situ* studies of Pt, Ru, Pd,[18] TiN,[19] and ZrN (Ref. 20) ALD films.

Cerium oxide nanostructures have been used for catalysis,[21] sensors, chemical mechanical planarization slurries,[22] and various biomedical applications.[21,23–25] Unique oxidative recycling properties of cerium oxide are the core reason for such diverse applications, although cerium oxide has also been used as high k-dielectric materials.[26] Thin film cerium oxide has also been used in semiconductor devices such as RAM.[27] According to the environment, oxidative cycling of Ce^{3+} and Ce^{4+} oxidation states has been utilized in many of the aforementioned applications. This unique behavior has been enhanced by nanodimensions, doping, different shapes, and morphologies. There are various ways to engineer defects into the structure to get their desired properties.[21] Atomic layer deposition is yet another technique to explore for the purpose.[28,29] However, ALD processes for cerium oxide are relatively few, with newer precursors being developed that demonstrate better stability, vapor phase transport, and deposition characteristics.[28–31] An effective and fast way of optimizing a cerium oxide ALD process is well desired among the community, which is the main objective of the current work.

Here, we demonstrate the rapid ALD process development of cerium oxide using precursor, $Ce(iPrCp)_2(N\text{-}iPr\text{-}amd)$ [bis-isopropylcyclopentadienyl-di-isopropylacetamidinate-cerium] (commercially know as Celine™) through *in situ* SE. Performed over a range of temperatures, a 3D visualization of the temperature window of the cerium oxide ALD process was created. This approach may serve as a useful process development tool for defining the ALD deposition characteristics, namely, its deposition rate as a function of temperature and pulse/purge times. The cerium oxide film properties were studied by x-ray photoelectron spectroscopy (XPS), x-ray diffraction (XRD), and atomic force microscopy (AFM), which showed excellent conformality and typical composition of cerium oxide ALD films.

II. EXPERIMENTAL DETAILS

A. Film deposition

Celine $[Ce(iPrCp)_2(N\text{-}iPr\text{-}amd)]$ precursor was procured from AirLiquide® and ultrapure analytical grade water (H_2O) was used as an oxidizer. Thin films were deposited in the Veeco®'s Fiji G2 system. This system is equipped with two ports on the opposite sides of the chamber wall for attaching the source and detector arms of an ellipsometer. A stainless-steel bubbler (Strem® 98-0271) was used to contain the Celine precursor. The Ar used to pressurize the bubbler was maintained at 68.94 kPa (10 psi) line pressure. The bubbler was kept at 145 °C to generate sufficient vapor pressure; valves and lines were kept at 155 °C to prevent any condensation. The manifold temperature was varied from 185 to 320 °C depending on experiments. Ultrapure nitrogen (N_2) gas was used as a carrier gas, and it is used to carry the Celine molecules to the main chamber and also to purge before and after an ALD cycle.

The approach used for rapid recipe development was the following. As opposed to alternate pulses of Celine and H_2O used in a traditional ALD recipe, a sequential precursor pulsing approach was adopted. In this approach, ten consecutive pulses of Celine, each measuring 2 s, were dosed inside the chamber first. Each Celine pulse was separated by a 5-s purge step. Next, ten consecutive pulses of water, each measuring 0.06 s, separated by 5-s purges, were dosed. The entire sequence of pulses can be denoted as ([2 s/5 s]10×)([0.06 s/5 s]10×). Throughout the dosing process, *in situ* ellipsometry was used to collect the deposition information. As shown in Fig. 1, a schematic diagram of the *in situ* ellipsometry aided ALD experiments.

At first, cerium oxide ALD precursor (Celine) pulse is introduced in the chamber, which leads to a change in thickness reading from *in situ* SE. Here, Celine is introduced in a pulsed manner to the ALD chamber. Assuming that (i) adsorption rate > desorption rate and (ii) multilayer adsorption mechanisms are not active, precursor molecules would be adsorbed on the substrate surface with each pulse, as illustrated in Fig. 1. We define θ_i as the fractional occupancy for adsorbed molecules on the available surface sites, where the subscript "i" corresponds to the pulse number. Thus, θ_i would change with each pulse. Moreover, during sequential pulsing, θ_1, θ_2, θ_3, …., should reach the maximum possible occupancy of available adsorption sites resulting in a full saturation of the surface. Following this, we would not see any change in thickness values with pulses of gases. As evident in Fig. 1 and more clearly in Fig. 2(b) (thickness versus time plot using *in situ* SE), a full saturation is achieved after the seventh pulse (14 s) for Celine; after the seventh pulse, we did not observe any appreciable change in the thickness. Similarly, water reacts with all surface sites after two pulses (0.12 s), and the thickness reaches saturation. As the reactant water pulse is introduced to the Celine saturated surface, the bulky organic ligands bonded to the cerium center are cleaved

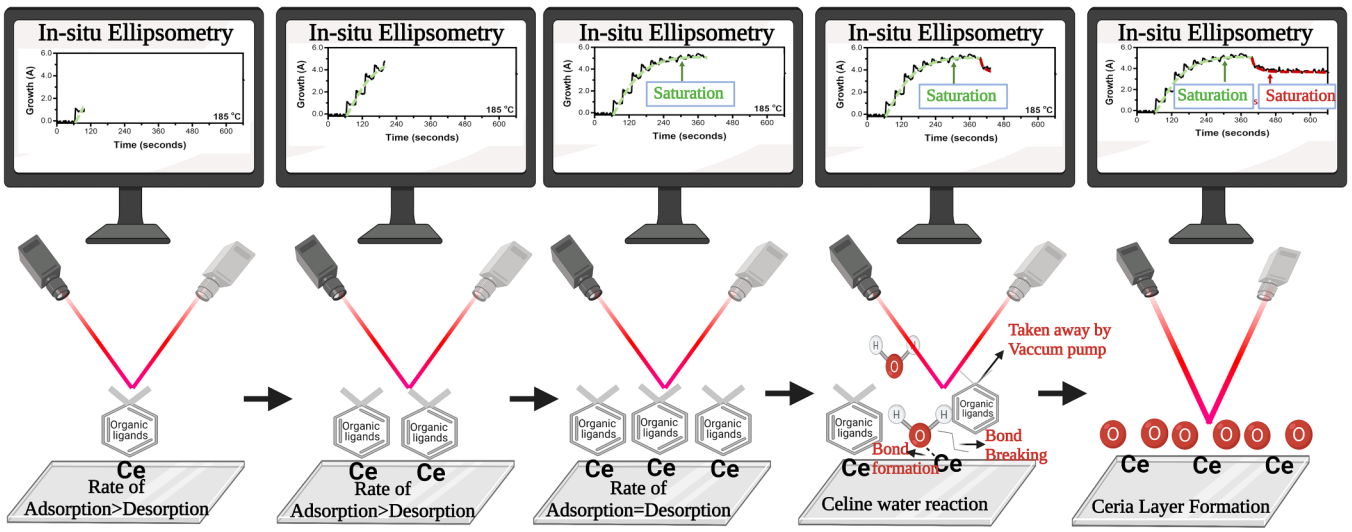

FIG. 1. Schematic diagram illustrating *in situ* ellipsometry experiments with the ALD process. The process begins with the sequential pulsing of Celine molecules, which get adsorbed on the surface of the substrate (silicon) that can be observed as the change in thickness showed by *in situ* SE of corresponding time, and the thickness of the adsorbed layer keeps on increasing until it reaches saturation (rate of adsorption = rate of desorption). After ten pulses of Celine, water (oxidizer) was introduced into the chamber in a pulsed manner. We have observed a decrease in thickness reading of *in situ* SE as the bulky organic ligands detach and the cerium oxide layer forms. After all the available sites are oxidized here, also we see saturation (no change in thickness reading with further water pulses).

to produce cerium oxide. A schematic is shown in Fig. 1. The removal of the ligands is observed as a slight decrease in total thickness value. This is consistent with previous reports that monitor ALD deposition with SE and QCM.[8,32]

B. Film characterization

In situ measurement of the thickness of ALD film was done using a spectroscopic ellipsometer from J. A. Woollam® M-2000 used at an incident angle of 69.5°, with a wavelength range from

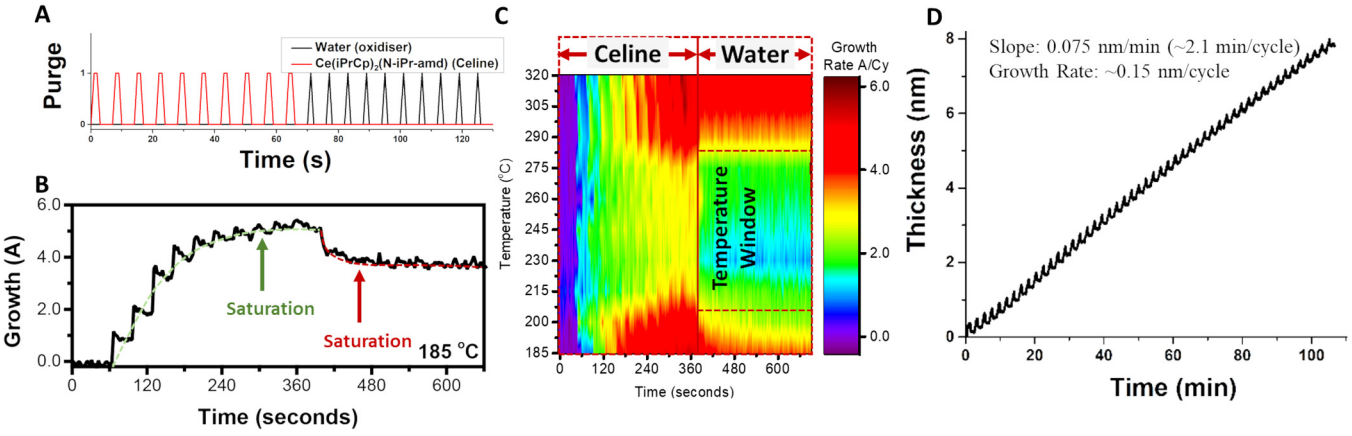

FIG. 2. *In situ* ellipsometry data of precursor-oxidizer saturation for cerium oxide ALD process optimization. (a) shows the precursor and oxidizer pulse and wait per cycle, Celine [$Ce(iPrCp)_2$(N-iPr-amd)] pulse of 2 s * 10× with 5 s wait between two consecutive pulses and similarly for water 0.06 s * 10× with 5 s wait between two consecutive pulses, as a whole represents one cycle; (b) shows the *in situ* ellipsometry thickness vs time plot for the experiment done at 185 °C, which clearly shows a saturation of thickness around the seventh Celine pulse and saturation of thickness around the second water pulse, and a deposition rate around 0.39 ± 0.01 nm per cycle (Å/Cy; 1 nm = 10 Å); (c) shows the contour plot highlighting change in the deposition rate with ALD process temperature and temperature window for self-limiting ALD process. The temperature was varied from 185 °C to 320 °C, and the deposition rate is indicated by the color which we could see first to decrease and then increase with temperature; (d) shows *in situ* ellipsometry data for 50 cycles at 245 °C. One cycle had 2 s * 7×with 5 s wait Celine pulses and 0.06 s * 2× with 5 s wait water pulses, in total 14 s of Celine pulse and 0.12 s of water pulse. We can see the linear deposition at ~0.15 ± 0.03 nm per cycle (at 245 °C).

190 to 1690 nm. The optical models for thin film analysis were built in the COMPLETE EASE software and consisted of an Si substrate with a native oxide of ~1.8 nm of SiO_2, followed by a Cauchy model for the cerium oxide top-layer, respectively. *In situ* values of Y and D are analyzed by COMPLETE EASE software and provide a simultaneous indication of saturation curves and deposition rate. Analysis of SE data based on the above model gave the film thickness and optical constants. It is important to note that all temperature-dependent saturation curves were performed sequentially on the same substrate, which prevented any deconvolution of optical constants at each deposition temperature. See the supplementary material[35] for full details of SE fitting parameters. PANalytical Empyrean system with grazing incidence capability was used to take x-ray diffraction pattern of thin films, and CuKα (1.54 Å) radiation was used as a source. XRD patterns were analyzed using X'PERT high-score software. An ESCALAB-250Xi XPS system was used to perform x-ray XPS. Experiments were done at a pressure below 7×10^{-9} mbar using Al-Kα monochromatic radiation, and the system was operating at a power of 300 W (15 kV, 20 mA). XPS data analysis and peak deconvolutions were done using THERMO AVANTAGE v5.9902 software (Thermo Fisher Scientific); binding energy was calibrated using the C1s peak (286.6 eV). Atomic force microscopy scans were done to see surface morphologies using a Veeco Dimension 3100 system. $5 \times 5\,\mu m^2$ area was scanned in the tapping mode with 512 lines per scan.

III. RESULTS AND DISCUSSION

The main outcomes from the *in situ* SE technique are shown in Fig. 2, where the key parameters of the ALD process were optimized using these outcomes.

A binary purge (0 = no purge; 1 = purge) versus time plot is shown in Fig. 2(a), and corresponding real-time ellipsometry (thickness versus time) is shown in Fig. 2(b). Real-time thickness values increase with every pulse of Celine until full surface saturation. As shown in Fig. 2(b), with every pulse of Celine, we can see an increase in thickness followed by a slight decrease in thickness value after the pulse, signifying adsorption, and desorption of precursors on the surface. With this one experiment, the saturation curve is defined. Repeating this experiment while varying the ALD chamber temperature by 15 °C from 185 to 320 °C, the deposition rate dependency of the temperature is revealed. The thickness per cycle at 185 °C is 0.39 ± 0.01 nm per cycle. The thickness per cycle decreases to 0.1 ± 0.01 nm per cycle at 230 °C. The deposition rate stays in the average 0.2 nm per cycle range in the temperature range of 215–275 °C and 0.15 ± 0.03 nm per cycle at 245 °C (temperature selected to run future process).

The information is better expressed in a temperature-time-deposition contour plot shown in Fig. 2(c). Here, the *x* axis serves as the time axis, whereas the temperature is shown on the y axis. The contour plot (given by the color scale) represents the deposition rate and varies from 0 to 0.6 nm/cycle. The demarcation between Celine and water doses is shown on the top *x* axis. The visualization is helpful as it aids in the determination of the "temperature window" for the given ALD process. Within the temperature window, deposition is stable not only as a function of temperature but also as a function of pulse time. This information is usually absent in the traditional approach adopted for reporting ALD processes, where only the data—deposition rate versus temperature—are plotted. By plotting the deposition rate in a multidimensional parameter space (temperature *and* pulse time), one can clearly visualize the temperature window during the water pulsing sequence. Here, the deposition rate is stable (~0.15 ± 0.04 nm/cycle) between 215 and 275 °C and rises to 0.35 ± 0.009 nm/cycle on either side of the window. The rise of deposition rates on the low temperature side can be attributed to precursor condensation effects, whereas the rise in deposition rates on the high temperature side can be attributed to precursor decomposition. We also note that the lowest deposition rate of 0.1 ± 0.01 nm/cy occurs at 230 °C. It is also to be noted that the ALD process is self-limiting, as is indicated by the stable deposition rate upon multiple sequences of either Celine or H_2O. See the supplementary material for Fig. S6,[35] a 3D plot representation for *in situ* ellipsometry data at different temperatures.

With the saturation curve and temperature window defined, the process parameters were kept constant to demonstrate the linear deposition with an increasing number of cycles. *In situ* SE data for 50 cycles of ALD run at 245 °C are shown in Fig. 2(d). The thickness deposition is linear as a function of ALD cycles. Here, the saw-tooth patterned deposition can be observed, showing the successive increase and then partial decrease of deposition due to the introduction of each reactant. The slope of the curve is 0.15 nm ± 0.03/cycle, which matches well with the observed deposition rate from the temperature-time-deposition plot in Fig. 2(c).

We note that Golalikhani *et al.* have previously reported the ALD of cerium oxide using Celine and water as precursors.[29] *Ex situ* studies were used to define the ALD deposition characteristics, namely, deposition rate as a function of pulse time, deposition rate as a function of purge time, linear deposition rate/thickness as a function of ALD cycles, and deposition rate as a function of temperature. Evident by the data points in their work, 21 experiments were performed to optimize the process. The deposition rate reported was 0.19 nm/cycle at a temperature of 240 °C. Compared to Golalikhani *et al.*, we show the same cerium oxide recipe development with a deposition rate of 0.15 ± 0.03 nm/cycle at 245 °C. However, we are also able to visualize minima in the deposition rate, as elucidated by Fig. 2(c), corresponding to 0.1 ± 0.01 nm/cycle at 230 °C. This deposition rate lies in a narrow temperature window, ~230 ± 5 °C. Traditional ALD approaches based on *ex situ* characterization can overlook finely spaced but important and localized deposition information. The ability to optimize processes in localized parameter spaces shows the power of performing *in situ* ALD process development.

We have observed a change in the deposition rate with temperature, as shown in Fig. 2(c). The higher deposition rate on either side of the temperature window (215–275 °C) can be attributed to the following factors: at low temperatures ($T < 215$ °C), physisorption of Celine may be favorable, leading to non-self-limiting deposition within the temperature window. Conversely, at the higher temperature, the Celine $(iPrCp)_2$(N-iPr-amd) ligands degrade, leading to conventional CVD deposition that is no longer self-limiting on the surface. These results are consistent with previous reports: Y_2O_3 ALD using $(iPrCp)_2$Y(iPr-amd) and Y$(EtCp)_2$(iPr-amd) precursors (with similar ALD precursor functional groups), where higher deposition rates were observed at temperatures due to decomposition of

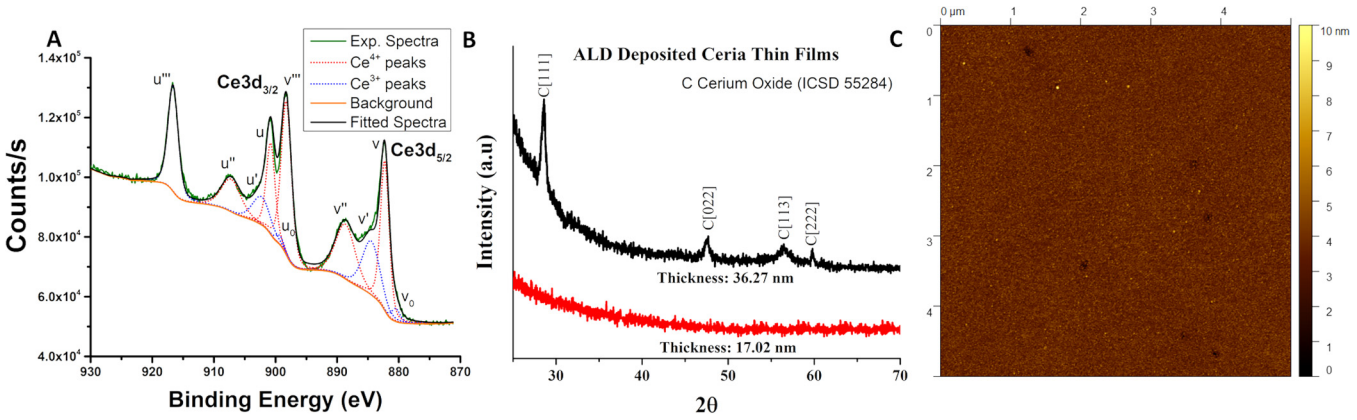

FIG. 3. XPS fit and deconvoluted spectral analysis of the surface Ce^{3+}, and Ce^{4+} oxidation states of 17.02 nm thick layer of ALD deposited cerium oxide. (a) GIXRD pattern of 17.02 and 36.27 nm thick cerium oxide thin films. No peaks are observed for the 17.02 nm cerium oxide (red/bottom). Although in 36.27 nm cerium oxide films, the diffraction peaks are observable and correspond to cerium oxide (ICSD 55284) (b). AFM height map of 17.02 nm cerium oxide film with a uniform roughness (rms) of 3.2 nm (c).

the ligands.[33,34] *In situ* SE data for thickness versus time for 50 cycles (precursor + water) is shown in Fig. 2(d); the film thickness continues to linearly increase after each cycle, which is characteristic of the ALD.[32] It is important to note that no nucleation delay was observed, which highlights the strong affinity for layer-by-layer deposition of cerium oxide on silicon.

Ex situ material characterization was performed on ALD deposited cerium oxide films. X-ray photoelectron spectroscopy on 17.02 ± 0.007 nm cerium oxide films indicate Ce^{3+} and Ce^{4+} oxidation states. As shown in Fig. 3(a) v_o, v', u_o, and u' (880.4, 884.6, 899.5, and 902.6 eV) peaks belong to Ce^{3+} oxidation state, and v, v'', v''', u, u'', and u''' (882.2, 888.8, 898.4, 900.7, 907.5, 916.7 eV) peaks belong to the Ce^{4+} oxidation state. Ce^{3+}/Ce^{4+} ratio was estimated using Ce3d scan. It was 0.255 ± 0.002, signifying $Ce^{3+} < Ce^{4+}$. See the supplementary material[35] for a detailed XPS analysis. Figure 3(b) shows the XRD of ALD deposited cerium oxide films. The 17.02 nm cerium oxide thickness sample did not exhibit peaks indicating that the film was amorphous. A thicker 36.27 ± 0.005 nm cerium oxide film exhibits all major peaks belonging to the cubic cerium oxide crystal system (fluorite structure with Fm3m space group; ICSD 55284), similar to earlier reports on cerium oxide ALD deposition.[28,29] The surface is characterized using AFM for surface topologies. The 17.02 nm cerium oxide film displays an RMS roughness of 3.2 ± 0.8 nm [Fig. 3(c)]. The *ex situ* characterizations substantiate the composition, phase, and conformality of the cerium oxide ALD films deposited at 245 °C. Subsequent materials characterization through XPS confirms the formation of the cerium oxide with relatively low surface roughness; an average roughness (rms) of 3.2 nm estimated from AFM scans indicate the relatively uniform layer. Earlier work with the same precursor also reported 8.13 and 1.72 nm average (rms) roughness of 300 nm ceria films deposited at 335 and 240 °C.[29]

It is important to highlight that the complete process development of Celine was accomplished after ten experiments. Compared to the 21 experiments previously used to develop this ALD process, the *in situ* approach accelerates process development time and reduces resource consumption while delivering better granularity in data in the process parameter space.[29] We have followed a stepwise approach that could be applied to any ALD process in general. These involve (i) identification of the saturation curves at each temperature from 185 to 320 °C (15 °C increments) using sequential pulsing of precursors; (ii) identifying and selecting an optimal process temperature within the temperature window; and (iii) demonstrating the linear deposition characteristics as a function of the number of cycles. This methodology saves time and resources and offers an advantage to monitor the deposition rate during operation.

IV. CONCLUSIONS

The ALD process development for cerium oxide [Celine (Ce(iPrCp)2(N-iPr-amd)) precursor and water as oxidizer] was done using *in situ* SE. At first, the saturation curve experiment was done to optimize the precursor, then oxidizer dosimetry, followed by repeating the same experiment with temperature variation. It enabled us to plot a contour plot of deposition rate versus temperature window from where we could extract critical ALD process parameters. For the cerium oxide ALD process, Celine precursor saturation was achieved in 14 s (2 s * 7 pulses); the optimal dose for water was 0.12 s (0.06 s * 2 pulses). The ALD temperature window was 215–275 °C, and 0.15 ± 0.04 nm/cycle average deposition rate in the temperature window, and linearity of deposition with respect to cycle numbers was also established using *in situ* SE data. Following this approach, optimization of saturation curves and temperature windows for controlled deposition rates can be done in as little as ten experiments, less than half the number of experiments that would be traditionally required. Further *ex situ* surface characterizations using AFM, XRD, and XPS have shown atomically smooth crystalline cerium oxide thin films with a cubic crystal structure.

ACKNOWLEDGMENTS

The authors would like to acknowledge SRC (GRC Task No. 3026.001) for providing funding for the research; the Materials

Characterizations Facility (MCF) and NSTC, UCF, for letting us use their characterizations facilities; and NSF MRI: ECCS (No. 1726636) for the HRXPS facility. C.F. was supported by the NSF under Award No. 1908167. BIORENDER software (Biorender.com) was used to create illustrative diagrams.

U.K. and C.F. contributed equally to this article.

DATA AVAILABILITY

The data that support the findings of this study are available from the corresponding authors upon reasonable request.

REFERENCES

[1]S. M. George, Chem. Rev. **110**, 111 (2009).
[2]S. Skoog, J. Elam, and R. Narayan, Int. Mater. Rev. **58**, 113 (2013).
[3]M. Leskelä and M. Ritala, Thin Solid Films **409**, 138 (2002).
[4]M. Leskelä and M. Ritala, Angew. Chem. Int. Ed. **42**, 5548 (2003).
[5]M. Leskelä, M. Mattinen, and M. Ritala, J. Vac. Sci. Technol. B **37**, 030801 (2019).
[6]O. Graniel, M. Weber, S. Balme, P. Miele, and M. Bechelany, Biosens. Bioelectron. **122**, 147 (2018).
[7]R. W. Johnson, A. Hultqvist, and S. F. Bent, Mater. Today **17**, 236 (2014).
[8]R. Matero, A. Rahtu, and M. Ritala, Chem. Mater. **13**, 4506 (2001).
[9]R. Matero, A. Rahtu, and M. Ritala, Langmuir **21**, 3498 (2005).
[10]J. W. Elam, M. D. Groner, and S. M. George, Rev. Sci. Instrum. **73**, 2981 (2002).
[11]X. Du, Y. Du, and S. M. George, J. Vac. Sci. Technol. A **23**, 581 (2005).
[12]S. B. S. Heil, P. Kudlacek, E. Langereis, R. Engeln, M. C. M. Van De Sanden, and W. M. M. Kessels, Appl. Phys. Lett. **89**, 131505 (2006).
[13]M. Juppo, A. Rahtu, M. Ritala, and M. Leskelä, Langmuir **16**, 4034 (2000).
[14]R. H. E. C. Bosch, L. E. Cornelissen, H. C. M. Knoops, and W. M. M. Kessels, Chem. Mater. **28**, 5864 (2016).
[15]S. Y. Lee, C. Jeon, S. H. Kim, Y. Kim, W. Jung, K.-S. An, and C.-Y. Park, Jpn. J. Appl. Phys. **51**, 031102 (2012).
[16]E. Langereis, H. C. M. Knoops, A. J. M. Mackus, F. Roozeboom, M. C. M. Van De Sanden, and W. M. M. Kessels, J. Appl. Phys. **102**, 083517 (2007).
[17]E. Langereis, S. Heil, H. Knoops, W. Keuning, M. Van de Sanden, and W. Kessels, J. Phys. D: Appl. Phys. **42**, 073001 (2009).
[18]N. Leick, J. Weber, A. Mackus, M. Weber, M. Van de Sanden, and W. Kessels, J. Phys. D: Appl. Phys. **49**, 115504 (2016).
[19]E. Langereis, S. B. S. Heil, M. C. M. Van De Sanden, and W. M. M. Kessels, J. Appl. Phys. **100**, 023534 (2006).
[20]T. Muneshwar and K. Cadien, Appl. Surf. Sci. **328**, 344 (2015).
[21]S. Seal, A. Jeyaranjan, C. J. Neal, U. Kumar, T. S. Sakthivel, and D. C. Sayle, Nanoscale **12**, 6879 (2020).
[22]M.-H. Oh, J.-S. Nho, S.-B. Cho, J.-S. Lee, and R. K. Singh, Powder Technol. **206**, 239 (2011).
[23]M. Doshi *et al.*, PLoS Neglected Trop. Dis. **14**, e0008654 (2020).
[24]J. Kieffer, S. Singh, B. S. Dhillon, U. Kumar, S. Shaikh, S. Ho, and S. Seal, Cureus **12**, e9675 (2020).
[25]S. Singh, U. Kumar, D. Gittess, T. S. Sakthivel, B. Babu, and S. Seal, J. Biomater. Appl. **2021**, 08853282211013451.
[26]S. Galata, E. Evangelou, Y. Panayiotatos, A. Sotiropoulos, and A. Dimoulas, Microelectron. Reliab. **47**, 532 (2007).
[27]M. Ismail, I. Talib, A. M. Rana, E. Ahmed, and M. Y. Nadeem, J. Appl. Phys. **117**, 084502 (2015).
[28]A. Gupta, T. S. Sakthivel, C. J. Neal, S. Koul, S. Singh, A. Kushima, and S. Seal, Biomater. Sci. **7**, 3051 (2019).
[29]M. Golalikhani, T. James, P. Van Buskirk, W. Noh, J. Lee, Z. Wang, and J. F. Roeder, J. Vac. Sci. Technol. A **36**, 051502 (2018).
[30]P. J. King *et al.*, Thin Solid Films **519**, 4192 (2011).
[31]Q. Lv, S. Zhang, S. Deng, Y. Xu, G. Li, Q. Li, and Y. Jin, Surf. Coat. Technol. **320**, 190 (2017).
[32]L. Lecordier, S. Herregods, and S. Armini, J. Vac. Sci. Technol. A **36**, 031605 (2018).
[33]I.-S. Park, Y. Chan Jung, S. Seong, J. Ahn, J. Kang, W. Noh, and C. Lansalot-Matras, J. Mater. Chem. C **2**, 9240 (2014).
[34]B. Zhao, F. Mattelaer, G. Rampelberg, J. Dendooven, and C. Detavernier, ACS Appl. Mater. Interfaces **12**, 3179 (2020).
[35]See supplementary material at https://doi.org/10.1116/6.0001329 for details about spectroscopic ellipsometry and XPS analysis.